Extracting Neutron Star Properties from X-ray Burst Oscillations

Nevin Weinberg*, M. Coleman Miller†, and Donald Q. Lamb*

*University of Chicago, Department of Astronomy and Astrophysics, 5640 South Ellis Ave., Chicago, IL 60637
†University of Maryland, Department of Astronomy, College Park, MD 20742-2421

Abstract. Many thermonuclear X-ray bursts exhibit brightness oscillations. The brightness oscillations are thought to be due to the combined effects of non-uniform nuclear burning and rotation of the neutron star. The waveforms of the oscillations contain information about the size and number of burning regions. They also contain substantial information about the mass and radius of the star, and hence about strong gravity and the equation of state of matter at supranuclear densities. We have written general relativistic ray-tracing codes that compute the waveforms and spectra of rotating hot spots as a function of photon energy. Using these codes, we survey the effect on the oscillation waveform and amplitude of parameters such as the compactness of the star, the spot size, the surface rotation velocity, and whether there are one or two spots. We also fit phase lag versus photon energy curves to data from the millisecond X-ray pulsar, SAX J1808–3658.

INTRODUCTION

Shortly after the launch of the *Rossi* X-ray Timing Explorer (RXTE) in late 1995, single kilohertz brightness oscillations were discovered in RXTE countrate time series data from thermonuclear X-ray bursts in several neutron-star low-mass X-ray binaries. These oscillations are remarkably coherent and their frequencies are very stable from burst to burst in a given source [1]. These oscillations are therefore thought to be at the stellar spin frequency or its first overtone. This suggests that the oscillations are caused by rotational modulation of a hot spot produced by non-uniform nuclear burning and propagation. Analysis of these oscillations can therefore constrain the mass and radius of the star and yield valuable information about the speed and type of thermonuclear propagation. In turn, this has implications for strong gravity and dense matter, and for astrophysical thermonuclear propagation in other contexts, such as classical novae and Type Ia supernovae.

A comparison of theoretical waveforms with the observations is required to extract this fundamental information. Here we exhibit waveform calculations that we have produced using general relativistic ray-tracing codes. We survey the effects of parameters such as the spot size, the stellar compactness, and the stellar rotational velocity, and demonstrate that our computations fit well the phase lag data from SAX J1808–3658.

COMPUTATIONAL METHOD

To compute observed light curves, we do general relativistic ray tracing from points on the surface to the observer at infinity in a way similar to, but more general than, [2] and [3]. For simplicity, we assume that the exterior spacetime is Schwarzschild, that the surface is dark except for the hot spot or spots, and that there is no background emission. The amplitudes would be reduced by a constant factor if there were background emission. The angular dependence of the specific intensity at the surface depends on both radiation transfer effects and Doppler boosting (see [4]). For each phase of rotation we compute the projected area of many small elements of a given finite size spot. We then build up the light curve of the entire spot by superposing the light curve of all the small elements. The grid resolution of the spot is chosen so that the effect of having a finite number of small elements can alter the value of the computed oscillation amplitudes by a fraction no larger than $\sim 10^{-4}$. After computing the oscillation waveform using the above approach, we Fourier-analyze the resulting light curve to determine the oscillation amplitudes and phases as a function of photon energy at different harmonics.

RESULTS

Panel (a) of Figure 1 shows the fractional rms amplitudes at the first two harmonics as a function of spot size and stellar compactness for one emitting spot centered on the rotational equator, as seen by a distant observer in the rotational plane. These curves demonstrate that a common result of the hot-spot model is large-amplitude brightness oscillations with a high contrast in strength between the dominant harmonic and weaker harmonics, as is observed in several sources. The curves for the first harmonic illustrate the general shape of most of the first harmonic curves. Initially, the amplitude depends only weakly on spot size. However, once the spot grows to an angular radius of $\sim 40°$ there is a steep decline in the oscillation amplitude which flattens out only near the tail of the expansion. This expected behavior appears to be in conflict with the decline in amplitude observed by Strohmayer, Zhang, & Swank (1997) from 4U 1728–34, in which the initial decline is steep. The cause of this could be that the initial velocity of propagation is large, or that the observed amplitude is diminished significantly by isotropization of the beam due to scattering (Weinberg, Miller, & Lamb 1999).

Panel (b) of Figure 1 shows the fractional rms amplitude at the second harmonic under the same assumptions but for two identical, antipodal emitting spots. The range in spot size here is $0° - 90°$ since two antipodal spots of $90°$ radii cover the entire stellar surface. Note that in this situation, there is no first harmonic.

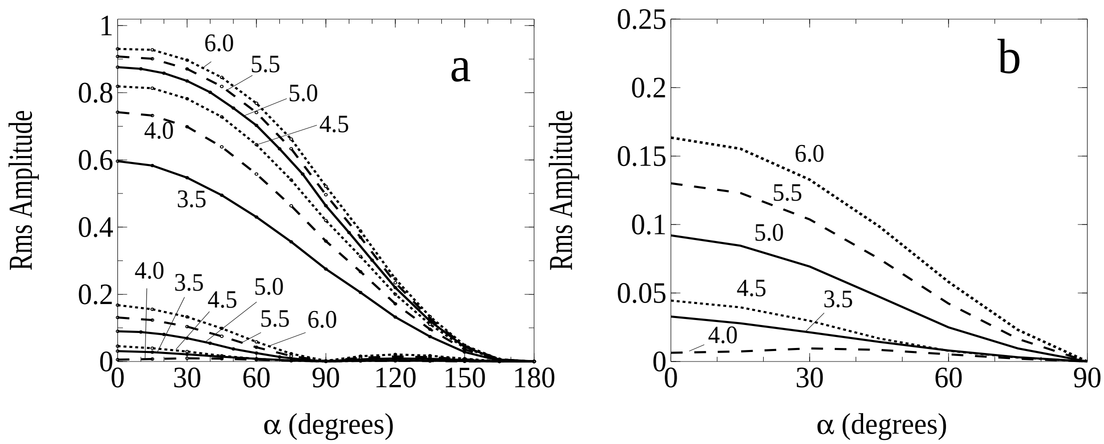

FIGURE 1. (a) Bolometric rms amplitude vs. the angular radius α of the spot at the first harmonic (upper curves) and the second harmonic (lower curves) from a single emitting spot centered on the rotational equator as seen by a distant observer in the rotational plane. Numbers denote values of R/M, where we use geometrized units in which $G = c \equiv 1$. (b) Rms amplitude vs. α at the second harmonic from two antipodal emitting spots, with both the spots and the distant observer in the rotational plane. Note the change in vertical scale in panel (b). In both cases we assume a nonrotating star and an isotropic specific intensity as measured by a local comoving observer.

These figures show that when there is only one emitting spot, the fundamental is always much stronger than higher harmonics. Thus, a source such as 4U 1636–536 with a stronger first overtone than fundamental [6] must have two nearly antipodal emitting spots. As described in detail in [4], we confirm the results of [2] and [3] that the rms amplitude decreases with increasing compactness until $R/M \approx 4$, then increases due to the formation of caustics. We also find that a finite surface rotational velocity increases the amplitude at the second harmonic substantially, while having a relatively small effect on the first harmonic (left panel of Figure 2).

As an application to data, in the right panel of Figure 2 we use our models to fit phase lag data from the millisecond accreting X-ray pulsar SAX J1808–3658. The waveforms from the accreting spot are expected to be similar to the waveforms from burst brightness oscillations, and the signal to noise for this source greatly exceeds that from burst sources such as Aql X-1 [7]. As is apparent from the figure, the fit is excellent. Further data, especially from a high-area timing mission, could be used to constrain the stellar mass or radius from phase lag data.

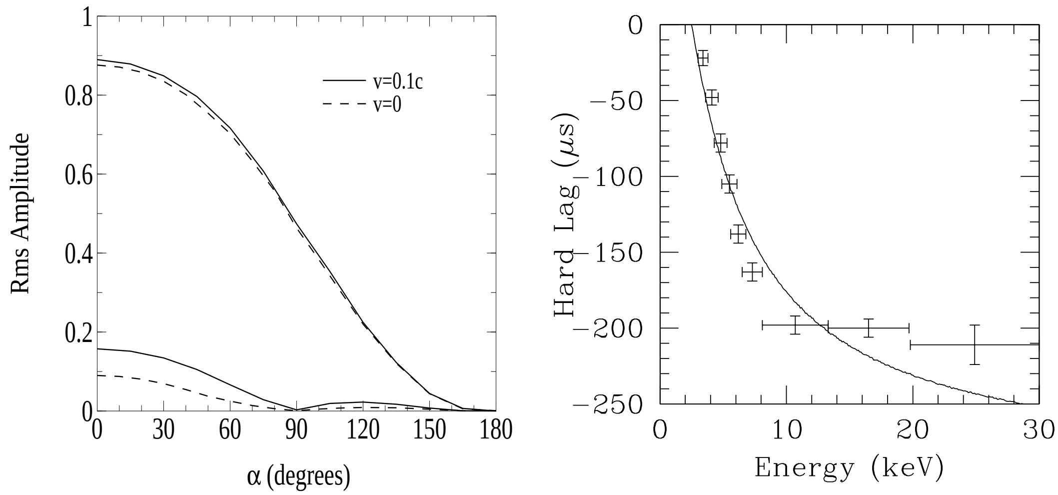

FIGURE 2. (left panel) Rms amplitude versus spot angular radius α at the first harmonic (upper curves) and the second harmonic (lower curves) from a single emitting spot with $v = 0.1c$ (*solid lines*) and $v = 0$ (*dashed lines*), $R/M = 5.0$, and a spot and a distant observer both in the rotational equator. (right panel) Phase lags versus photon energy for the millisecond X-ray pulsar SAX J1808–3658. The data (crosses) are from [8], where the reference energy is the 2–3 keV band. The solid line shows the phase lags in a Doppler shift model, assuming a gravitational mass of $1.8\,M_\odot$ and a rotational velocity of 0.1 c as measured at infinity, which would be appropriate for the observed 401 Hz spin frequency and $R = 11$ km. The angular and spectral emission at the surface are that of a grey atmosphere with an effective temperature of 0.6 keV as measured at infinity. The excellent fit apparent in this figure supports the Doppler shift explanation for the soft lags in this source.

REFERENCES

1. Strohmayer, T. E., Swank, J. H., & Zhang, W. 1998 (astro-ph/9801219)
2. Pechenick, K. R., Ftaclas, C., & Cohen, J. M. 1983, ApJ, 274, 846
3. Miller, M. C., & Lamb, F. K. 1998, ApJ, 499, L37
4. Weinberg, N., Miller, M. C., & Lamb, D. Q. 1999, in preparation
5. Strohmayer, T. E., Zhang, W., & Swank, J. H. 1997, ApJ, 487, L77
6. Miller, M. C. 1999, ApJ, 515, L77
7. Ford, E. C. 1999, ApJ, 519, L73
8. Cui, W., Morgan, E. H., & Titarchuk, L. G. 1998, ApJ, 504, L27